

# LHC RUN-III CONFIGURATION WORKING GROUP REPORT

N. Karastathis\*, M. Barnes, H. Bartosik, K. Brodzinski, X. Buffat, F. Cerutti, S. Fartoukh†, B. Goddard, G. Iadarola, S. Le Naour, A. Lechner, J. Maestre Heredia, A. Mereghetti, E. Metral, D. Missiaen, N. Mounet, F.X. Nuiry, S. Papadopoulou, Y. Papaphilippou, B. Petersen, C. Schwick, G. Rumolo, B. Salvant, M. Solfaroli Camillocci, G. Sterbini, H. Timko, R. Tomas Garcia, J. Uythoven, J. Wenninger  
CERN, CH-1217 Meyrin, Switzerland

## Abstract

After its second successful run period, the Large Hadron Collider (LHC) [1] shuts down for two years with the plan of being recommissioned in 2021 for a three-year physics production period, the Run-III. The future restart of the LHC coincides with the completion of the LHC Injectors Upgrade (LIU) project [2], offering to the LHC the opportunity and the challenge to operate with up to two times higher beam brightness. For this purpose, the LHC Run-III Configuration Working Group (LCR3) was formed to identify the limitations on the various LHC systems, and seek possible mitigations or constraints in terms of the accepted beam parameters. The LCR3 is in charge of establishing operational scenarios and estimating them in terms of their integrated performance. These proceedings summarize the status of the working group, highlight the known constraints and suggest a preliminary version of the LHC cycle in Run-III.

## INTRODUCTION

Planning the operational scenarios for the third run period of the LHC, the LCR3 working group focused on identifying possible limitations of the LHC systems, arising by the foreseen performance of the LIU and its deliverable beam parameters. A maximum acceptable bunch intensity was overall agreed and the stable operation was scrutinized in terms of optics parameters, coherent stability and beam lifetime.

One of the major concerns for the Run-III operation is the preservation of the luminosity lifetime of the inner triplets at the two high-luminosity experiments (interaction points IP1 [3], IP5 [4]). Two optics regimes were identified and evaluated in terms of their performance and ease of commissioning. Additional constraints from the lower luminosity (IP2 [5], IP8 [6]) and the Forward Physics (AFP [7], CTPPS [8]) experiments required an almost global re-design of the LHC cycle optics.

Considering all the limitations in terms of equipment and beam dynamics, preliminary operational scenarios were developed, with the foreseen integrated performance exceeding  $210 \text{ fb}^{-1}$  for IP1 and IP5,  $216 \text{ pb}^{-1}$  for IP2 and  $31 \text{ fb}^{-1}$  for IP8, in the years 2021-2023 of the Run-III period.

These proceedings present the status of the Run-III study at the time it was presented. Several numbers are used as preliminary, such as the beam collision energy of 7 TeV,

since the final decision is pending approval by the LHC Machine Committee.

## LIU & LHC SYSTEMS LIMITATIONS

The LIU Project includes the full LHC injectors chain (LINAC4 [2], PS Booster, PS and SPS [9]). Several upgrades [10] in all injector machines will significantly improve the brightness of the beam injected into the LHC. The well-established injectors commissioning plan consists of a gradual ramp-up throughout the duration of Run-III. The maximum LHC injected bunch intensity is estimated to be  $1.4 \times 10^{11}$  ppb by the end of 2021, to  $1.8 \times 10^{11}$  ppb by the end of 2022, and up to  $2.1 \times 10^{11}$  ppb by the end of 2023. The LIU ramp-up will continue in 2024 up to the High Luminosity LHC (HL-LHC) [11] target of  $2.3 \times 10^{11}$  ppb, but the LHC will not follow as in 2024 the third LHC Long-Shutdown period (LS3) is scheduled to start.

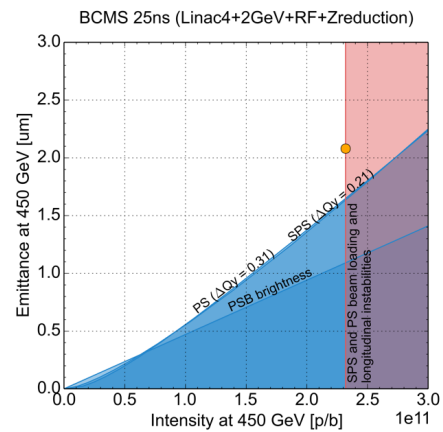


Figure 1: The performance reach of the LIU BCMS beams at the SPS extraction.

Following this plan, during Run-III, the LHC should profit as much as possible from the brighter beams delivered. The BCMS [12] beam is considered as baseline, since it features a smaller emittance at injection which should lead to less losses in the transfer line, on the injection plateau, and during the ramp of the LHC. In addition, the BCMS scheme can also mitigate by about 10 % the cryo-cooling capacity needed to cope with the heat load generated by the electron cloud (e-cloud) in the LHC arcs. The brightness curve of the BCMS beam is shown in Fig. 1. The first mandate of the LCR3 working group is to identify whether the LHC systems can

\* nikolaos.karastathis@cern.ch

† stephane.fartoukh@cern.ch

safely inject, accelerate, collide and dump injected beams with the aforementioned parameters.

### *Injection Kickers*

The injected beam passes through 5 horizontally deflecting steel septum magnets (MSI) and four vertically deflecting kickers (MKIs) [1]. The power dissipated in the ferrites consisting of the MKI depends on the beam parameters (total intensity and bunch length), on the magnet beam coupling impedance and on the available cooling mechanisms. The limiting magnet (MKI 8C) in the present system is expected to restrict the bunch intensity to  $1.5 \times 10^{11}$  ppb with a bunch length of 1.1 ns and 2592 bunches, assuming a Gaussian longitudinal distribution. Further studies [13] with 2808 equidistant bunches with Gaussian longitudinal profile show that the intensity of  $1.8 \times 10^{11}$  ppb is achievable in the LHC with a bunch length of  $\approx 1.3$  ns in permanent regime. This means that a bunch population of  $1.8 \times 10^{11}$  ppb could in principle be sustained only for a couple of hours or more, depending upon the temperature of the ferrite yoke at the start of the fill without exceeding the MKI temperature limit, while assuming a reduced bunch length. This parameter will be chosen later on to 1.2 ns (instead of 1.0 ns in the LHC and as for the HL-LHC), and will be adjusted depending on the need in Run-III. Finally, a new MKI prototype is planned to be installed during LS2, in the injection region at IP2, to be validated with beam. If the validation is successful, the other three MKI magnets at IP2 will be exchanged by the end of 2022-2023 Year End Technical Stop (YETS).

### *Radio-Frequency System*

The injected beam is captured, accelerated and stored using the 400 MHz superconducting cavity system [1]. The klystrons are rated to deliver 300 kW of RF power, but in operation the observed readings reveal a saturation at 250–280 kW, although with large error-bars. Several studies in the machine (MD) [14] have been performed during Run-II to identify the optimal settings to improve the SPS-LHC matching and reduce the power consumption for the LIU beams. A beam with bunch intensity of  $1.8 \times 10^{11}$  ppb can be injected in the LHC by setting the RF voltage at 6.4 MV, while guaranteeing a good RF capture in the LHC using the SPS Q20 optics [15]. The RF power consumption is independent of beam current during acceleration and flat top thanks to the full-detuning beam-loading compensation scheme. At the targeted energy of 7 TeV, the present system is fully potent to operate at the required 16 MV for  $\approx 1.2$  ns long bunches, as targeted to ease the controlled emittance blow-up in the ramp.

### *Cryogenics*

The LHC superconducting magnet windings (arcs, dipole suppressors and inner triplets) are immersed in a bath of superfluid helium at a pressure of about 0.13 MPa and a maximum temperature of 1.9 K [1]. The guaranteed value for cryogenic capacity for the inner triplets in IR1 and IR5 for dynamic heat load compensation was measured at

270 W (306 W for total heat load). Within this capacity, a maximum luminosity of  $2.2 \times 10^{34}$  Hz cm<sup>-2</sup> at 6.5 TeV or  $2.05 \times 10^{34}$  Hz cm<sup>-2</sup> at 7 TeV [16] can be maintained. In case of luminosity leveling, the impact of operating the inner triplets at the cryogenics limit is marginal ( $\approx 2\%$ ) on the cooling capacity of the beam screens in the adjacent arcs.

### *Beam Dump Systems*

The LHC beam dump system of each ring consists of 15 extraction kicker magnets (MKD), 15 steel septum magnets (MSD) and 10 modules of dilution kicker magnets (MKB). While no issues have been identified for the extraction kickers, installing two additional modules to the MKB system will increase the failure safety margin [17]. The most critical components of the system, affected by the increased intensity, are the main dump (TDE assembly and its upstream and downstream windows), the septum and main ring protection devices, TCDS and TCDQ respectively. The overall system was initially designed to withstand bunch intensities up to  $1.7 \times 10^{11}$  ppb.

Concerning the TDE assembly, the core is made of low and high density graphite segments with a sublimation temperature expected to be above 3000 °C. This temperature is reachable with the full HL-LHC beams (or 2400 °C for  $1.8 \times 10^{11}$  ppb) if two MKB's do not fire. A re-characterisation of the core material is required to guarantee this bunch intensity. The TDE downstream window, made of TiGr<sub>2</sub>, cannot withstand the HL-LHC beams, but an exchange of the window is planned for LS2, removing the constraint for Run-III operation. However, the upstream window of the TDE, made of CfC and steel layers, has no sufficient margin for the full HL-LHC beams and therefore is a limitation on the bunch intensity targeted in Run-III [18]. A complete re-design is foreseen for the YETS 2021/2022 in order for the upstream window to be compatible with the bunch intensity of  $1.8 \times 10^{11}$  ppb.

The two existing TCDS absorber modules are not expected to be a limitation for Run-III, as they were initially designed for bunch intensities up to  $1.7 \times 10^{11}$  ppb with enough safety margin. The results will be re-confirmed with a second iteration of the simulations for a bunch intensity of  $1.8 \times 10^{11}$  ppb. Finally, the TCDQ absorber was already upgraded in LS1 considering the full HL-LHC beam parameters, for which the load was well within the material limits. However, during Run-II, new MKD erratics (Type-2) have been observed, during which the particle density hitting the TCDQ could be higher than expected, thus limiting the minimum possible TCDQ half-gap. Further thermo-mechanical simulations with 2.5 mm half-gap revealed that an intensity of  $1.7 \times 10^{11}$  ppb is reachable with a safety factor of at least 2.0 [19]. Since the TCDQ half-gap can be a limiting factor of the minimum achievable  $\beta^*$  in the high luminosity IPs, additional studies are on-going with different values of half-gap.

## Alignment

A magnet alignment campaign takes place during every long shutdown to re-align the magnets and to provide an optimal design trajectory. The experiment hosted in IR5 requested a re-alignment of the LSS5, which is the long straight section in IR5, during LS2. A vertical re-alignment of up to  $-3$  mm is scheduled [20]. The outcome of the campaign does not impact the maximum bunch intensity accepted in the LHC, but it could be a constraint to the optics design.

## Collimation System

The LHC collimation system provides an efficient cleaning of the beam halo during the full LHC cycle. A major upgrade of the system is foreseen for the LS2 and LS3 periods to significantly decrease the contribution of the collimators to the impedance budget of the ring. While the collimation settings in Run-III will be similar to the 2018 run period in order to protect the inner triplets, there is no concern in finding appropriate settings for bunch intensities up to  $2.5 \times 10^{11}$  ppb [21].

Collecting all the concerns of the various LHC systems, the maximum bunch intensity acceptable during Run-III is limited to  $1.8 \times 10^{11}$  ppb. Comparing with the LIU commissioning plan, the LHC could, in principle, follow the LIU beam intensity ramp-up until the end of 2022, but not accept more than  $1.8 \times 10^{11}$  ppb in 2023.

## BEAM PHYSICS CONCERNS

Operating with a maximum bunch intensity 50 % higher than that of Run-II can have significant impact on the beam dynamics of the LHC. The three major concerns, even before the collision process begins, are the emittance blow-up, the coherent stability and the heat load generated in the two rings.

### Emittance Blow-Up

The two major mechanisms that affect the emittance evolution along the cycle are the Intra-Beam Scattering (IBS) and the Synchrotron Radiation (SR). On the injection plateau, with a beam energy of 450 GeV, the IBS is the dominant process resulting in an increase of the horizontal emittance and of the bunch length, due to dispersion. The contribution of SR results in a damping of the vertical emittance. Figure 2 shows the estimated effect on the transverse and longitudinal emittances of a beam with a bunch intensity of  $1.8 \times 10^{11}$  ppb, a normalized transverse emittance of  $1.3 \mu\text{m}$  and a  $4\sigma$  bunch length of 1.2 ns. These estimates are drawn from IBS and SR modelling [22] performed for two cases of the injection RF voltage. Additional mechanisms that can affect the emittance evolution throughout the LHC cycle, such as e-cloud had not been considered in these estimates.

The injection at the LHC lasts  $\approx 40$  min. Based on these estimates, the horizontal emittance grows to  $1.65 \mu\text{m}$  at the start of the ramp. During Run-II an emittance blow-up was observed during the ramp process [23]. Considering two

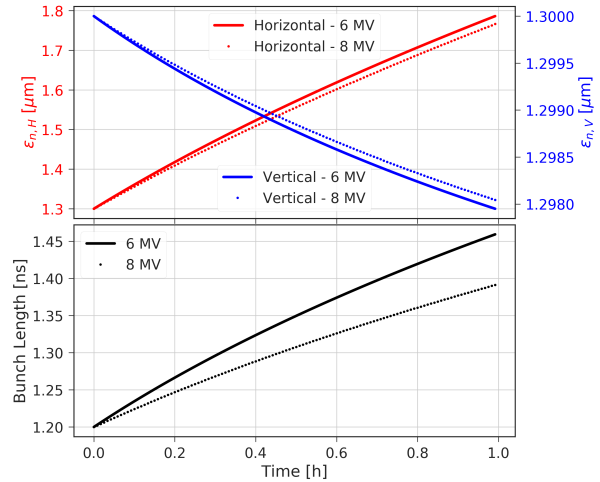


Figure 2: Estimated evolution of emittances (transverse and longitudinal) on the injection plateau energy of 450 GeV for a beam with initial conditions of  $1.8 \times 10^{11}$  ppb,  $1.3 \mu\text{m}$  normalized transverse emittance and  $1.2$  ns  $4\sigma$  bunch length. The estimates are performed with two values of RF klystron voltage.

extreme values, the emittance at the start of collisions can be assumed in the range of  $1.8 - 2.5 \mu\text{m}$ . In terms of bunch length at the start of collisions, a  $4\sigma$  of  $\geq 1.2$  ns can be envisaged and is preferred by the RF and MKI systems.

### Heat Load

A challenge for LHC operation with 25 ns in Run-II was the total load on the cryogenics plants, dominated by the beam induced heating on the beam screens of the arcs. During Run-II, each of the 8 sectors of the LHC ring, had a different response in terms of heat load [24]. This behaviour was not observed during Run-I, pointing to a degradation during LS1. Understanding and avoiding further degradation during LS2 is crucial in view of the Run-III.

The beam induced heating shows a strong dependence on the bunch spacing of the filling scheme. Observations during LHC operation in Run-I and II, revealed a large increase in the specific heat load when operating with 25 ns compared to 50 ns bunch trains. Since the impedance and SR do not depend on the filling scheme, the e-cloud is the only identified mechanism compatible with these observations [24]. The operational configuration during Run-II was to spend the available cryogenics margin to mitigate the e-cloud. However, since the heat load depends on the bunch intensity, by increasing the bunch intensity in Run-III, the additional cryogenics margin reduces significantly. As far as the e-cloud is concerned, the LHC sectors can be categorized into high load sectors (S78, S81, S12, S23, especially S12 and S23) and low load sectors (S34, S45, S56, S67) when the average Secondary Electron Yield (SEY) parameter is 1.35 and 1.25, respectively. Figure 3 shows the heat load contributions for a high load sector for a BCMS 25 ns beam. The cryogenics limit of  $\approx 10$  kW/arc in the high load sectors

is at the limit of the total heat-load contributions expected for a bunch intensity of  $1.8 \times 10^{11}$  ppb.

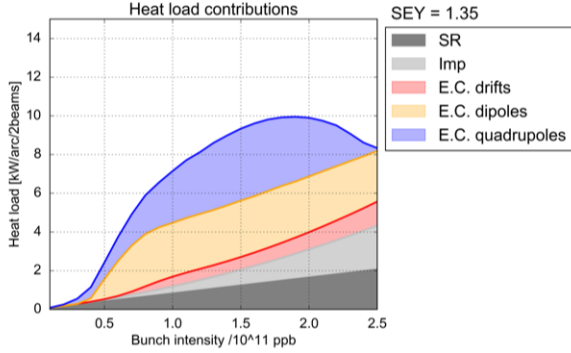


Figure 3: Estimated contribution of various sources on heat load of a sector with SEY of 1.35 as a function of the bunch intensity. The BCMS beam is considered here. The maximum cryogenics capacity of  $\approx 10$  kW/arc is expected to be reached with a bunch intensity of  $1.8 \times 10^{11}$  ppb.

In case of further degradation during LS2, an e-cloud mitigation technique easily implemented is the change of the filling scheme. The combination of 25 ns BCMS trains together with 8b+4e [12] trains could in principle provide up to 25 % of missing cryo-cooling capacity at the expense of only 9 % less collisions in IP1/5. Figure 4 shows a schematic of the BCMS and the alternative mixed filling scheme that provides 2736 and 2484 collisions in IP1/5, respectively. Mixed filling schemes had been only used in MDs during Run-II, but they are also viable during nominal operation, since the injectors provide two types of beams ("nominal" and "intermediate") per hyper-cycle. In case a third beam is required to be injected in the LHC (e.g. the pilot, together with the BCMS and 8b+4e beams) a change of the hyper-cycle is required with the present system, which might result in a slight increase of the turnaround time until the procedure is fully automatized.

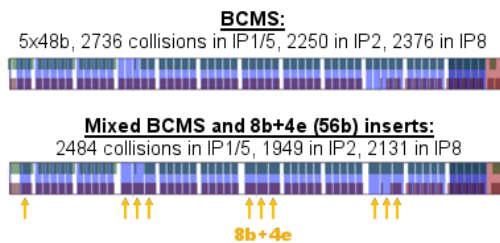


Figure 4: Two filling schemes are considered for the operation during Run-III. The first one is a pure BCMS, resulting in 2736 collisions in the two high luminosity experiments. The second one is a mixed filling scheme, that consists of BCMS beams with 8b+4e inserts to gain back some cryogenics capacity margin by mitigating the e-cloud production. This results in 2484 collisions at IP1/5.

## Coherent Stability

The coherent stability greatly depends on the impedance of the machine. Several upgrades scheduled during LS2 [21] will significantly improve the transverse impedance. To maintain coherent stability, the chromaticity is set to a high value ( $\approx 15$ ) to minimize the growth rate of instability modes. These modes are then stabilized by Landau damping originating essentially from the transverse tune spread, the main source of which being the octupole magnets (as long as head-on collisions do not occur, i.e. before stable beams are declared). Finally, the transverse damper (ADT) [25] is also used as an on-line transverse instability mitigation method. Since the octupole detuning coefficients are weighted by the  $\beta$  function in the arcs, the efficiency of the octupoles can be enhanced using proper optics settings.

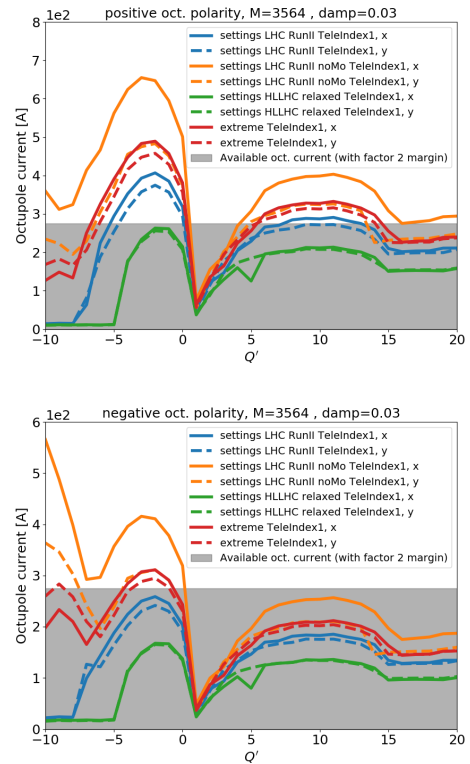


Figure 5: The octupole threshold at 7 TeV as a function of the chromaticity for different collimation settings scenarios. The results consist of both the positive (top) and negative (bottom) octupole polarity.

Figure 5 shows the octupole thresholds at 7 TeV beam energy, for both octupole polarities, as a function of the chromaticity for various collimator settings scenarios, in the presence of the ADT. The results are given for a beam brightness of  $1 \times 10^{11}$  ppb/ $\mu\text{m}$ , but the long-range beam-beam effects are not considered. In addition, a safety factor of 2 is included, as observed experimentally to account for other effects, such as noise. While the collimator upgrade significantly improves the stability, reaching the same octupole threshold of 150-200 A (not including the safety factor of 2)

as in Run-II, would require to use the telescopic optics [26] with a telescopic index of 2.5. The negative polarity also gets compensated by the long-range beam-beam detuning, which is beneficial in terms of dynamic aperture, but detrimental for stability, hence with this polarity the situation is more critical than visible in Fig. 5. To allow for further optimization, both octupole polarities should be kept operational, which stresses the need for deploying a telescopic index already in the ramp to allow for any beam-beam separation.

## OPTICS AND TRIPLET LIFETIME

The major concern for the Run-III operation is the luminosity lifetime of the inner triplets in IR1 and IR5, which are scheduled for replacement in LS3. Their estimated maximum dose is 30 MGy. Studies during the lifespan of the triplets have identified two highly irradiated coils, Q2a in IR1 and Q2b in IR5 [27], with the former being the overall limiting coil. At the  $190 \text{ fb}^{-1}$  already collected during Run-I and Run-II, the IR1 Q2a is estimated to have already collected 13 MGy, and IR5 Q2b 11 MGy, which bring them almost half-way of their life.

The irradiation of various azimuthal locations of the triplet coils in the transverse plane depends heavily on the choice of the crossing angle (polarity, magnitude and crossing plane). For Run-III, two optics configurations can be thought as possible candidates for operation. The first one is the well-known round optics in which the  $\beta_{\text{round}}^*$  at the crossing plane of each IP, namely  $\beta_X^*$  is equal to the one in the parallel plane, namely  $\beta_{\parallel}^*$ . This has already been used throughout Run-I and Run-II. Round optics provide the freedom to reverse the polarity on the vertical crossing plane and thus irradiating different azimuthal locations. This reversal had already been exploited during Run-II resulting to an overall decrease of the peak dose by 30 %.

The second configuration is the flat optics. As shown in Fig. 6, the  $\beta^*$  function in the parallel plane,  $\beta_{\parallel}^*$ , is smaller than that in the crossing plane  $\beta_X^*$ , but it holds that  $\sqrt{\beta_X^* \cdot \beta_{\parallel}^*} \approx \beta_{\text{round}}^*$  at constant luminosity. For this scheme to be compatible with the LHC, an exchange of the crossing planes in IP1/5 is required due to the beam screen shape. In terms of peak dose, the flat optics provide a decrease of 35 %, since different locations of the coils are irradiated.

Finally, another important element affecting the triplet dose is the absolute value of the crossing angle at the IP. Fig. 7 shows a comparison in terms of peak dose around IR1 for a scenario of operating with round optics with half-crossing angle of  $160 \mu\text{rad}$  and  $110 \mu\text{rad}$ , as well as the case of operating with flat optics with  $110 \mu\text{rad}$ . The results suggest that flat optics can be an appealing option for reducing the peak dose, but also that operating with smaller crossing angle is beneficial in terms of triplet irradiation. Therefore, the target of any operational scenario for Run-III would be to keep the crossing angle as small as possible during a fill, without sacrificing beam performance.

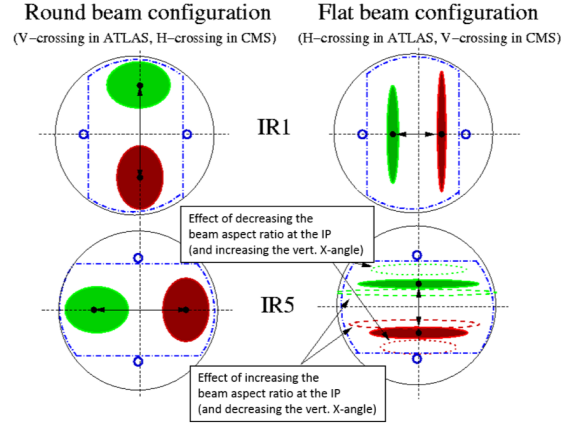


Figure 6: A schematic from Ref. [28] showing the configurations for the IR1/5 beam footprints in the inner triplet in the case of round (left) and flat (right) optics. A swap of the crossing planes between the two IRs is required for the flat optics configuration due to the shape of the beam screen.

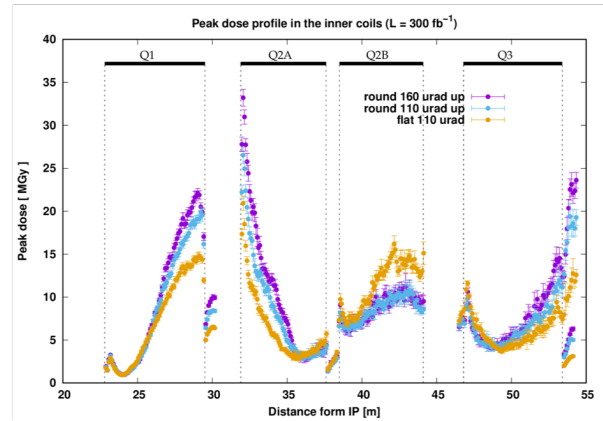


Figure 7: Simulation results of the peak dose as a function of the distance from IR1. The scenarios studied include two round optics configurations with different values of half-crossing angle and one with flat optics. A reduction of the peak dose is observed for the flat optics, as well as in the round configuration with the smaller crossing angle.

## Constructing Running Scenarios considering Beam-Beam Effects

The lower limit on the crossing angle is imposed by the beam-beam interactions. To estimate these effects, Dynamic Aperture (DA) simulations have been run. Such simulations have been used extensively during Run-II to guide the LHC operation in various occasions, as for example for the crossing angle anti-leveling [29] implemented in 2017 and 2018 in the LHC.

In the regime of optimal working point (WP), the bunch intensity is linearly correlated to the normalized crossing angle for keeping the same DA, as shown in Fig. 8 for a  $\beta^*$  of 0.8 m and a telescopic index of 2.5. Restricting the luminosity at  $2 \times 10^{34} \text{ Hz cm}^{-2}$  and considering the machine

Min DA LHC Run-III,  $r_{ATS}=2.5$ ,  $\beta^*=80\text{cm}$ ,  $(Q_x, Q_y)=(62.313, 60.318)$   
 $\epsilon_n=2.50\mu\text{m}$ ,  $Q=15$ ,  $I_{M0}=+350\text{A}$ ,  $L_{IP8}^{\text{ev}}=2 \cdot 10^{33} \text{ Hz/cm}^2$

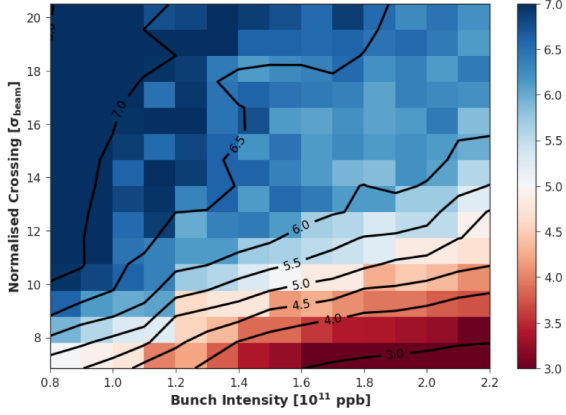


Figure 8: Correlation between the normalized crossing angle and bunch intensity. For well optimized working point an almost linear correlation is identified.

aperture, the half-crossing angle can be adapted as a function of the  $\beta^*$ . This evolution is shown in Fig. 9, where initially the half-crossing angle is kept small (109  $\mu\text{rad}$ ) and increased to the aperture limit (162  $\mu\text{rad}$ ) as the  $\beta^*$  is squeezed from 1.2 m to 0.28 m. In the same figure, the evolution of the intensity as a function of  $\beta^*$  is shown under four different combinations of the normalized emittance and number of bunches. This reveals that depending on the initial intensity delivered in the LHC, a large dynamic range of  $\beta^*$  values has to be accommodated.

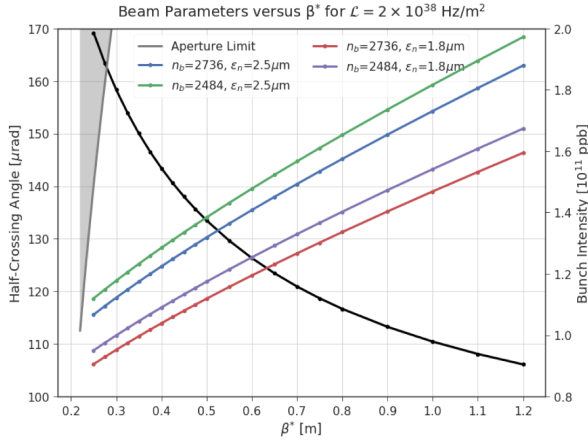
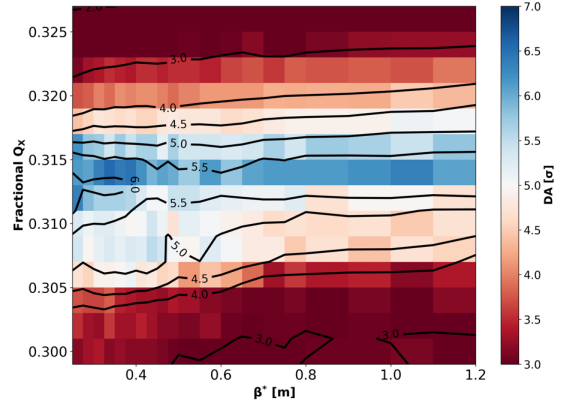


Figure 9: Evolution of the half-crossing angle as a function of the  $\beta^*$  (black curve) when leveling the luminosity to  $2 \times 10^{34} \text{ Hz cm}^{-2}$ . Different scenarios in terms of number of bunches and transverse emittance at the start of collisions reveal the need to deploy optics that can cover a large range of initial  $\beta^*$ .

This parametric scheme was evaluated in terms of DA and is shown in Fig. 10. Assuming a tune split of  $5 \times 10^{-3}$  and the linear coupling corrected to  $10^{-3}$  level to avoid the loss of Landau damping, an optimal working point kept almost constant along the fill, can be found (in this case (62.313,

60.318)), which can ease operation. Furthermore, the variation of the crossing angle with  $\beta^*$ , to level the luminosity at the target value, yields a DA above  $5.5\sigma$  for both 2736 and 2484 colliding bunches. The additional DA above the target of  $5\sigma$  could be used to further reduce the crossing angle or to accommodate the effect on DA of diffusive effects currently not included in the simulation model (e.g. e-cloud).

Min DA LHC Run-III,  $r_{ATS}=1.6$ ,  $n_b=2736$ ,  $\epsilon_n=2.5\mu\text{m}$ ,  $Q=15$   
 $Q_y=Q_x+0.005$ ,  $I_{M0}=+500\text{A}$ ,  $L_{IP8}^{\text{ev}}=2 \cdot 10^{33} \text{ Hz/cm}^2$



Min DA LHC Run-III,  $r_{ATS}=1.6$ ,  $\epsilon_n=2.5\mu\text{m}$ ,  $Q=15$   
 $(Q_x, Q_y)=(62.313, 60.318)$ ,  $I_{M0}=+500\text{A}$ ,  $L_{IP8}^{\text{ev}}=2 \cdot 10^{33} \text{ Hz/cm}^2$

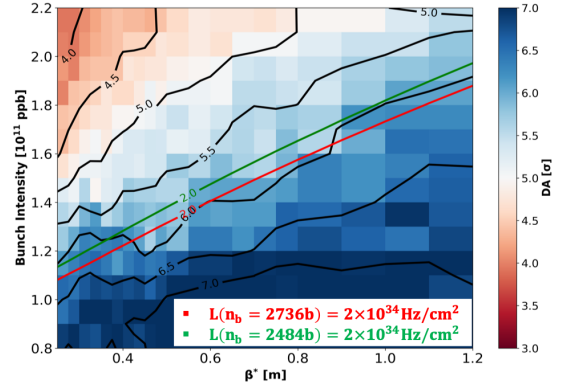


Figure 10: Minimum DA as a function of the working point, moving along the diagonal with a tune split of  $5 \times 10^{-3}$ , and the  $\beta^*$  (top), and idem replacing the WP by the bunch population (bottom). The crossing angle is fixed in each  $\beta^*$  following the curve of Fig. 9. In the top plot the luminosity is kept constant at  $2 \times 10^{34} \text{ Hz cm}^{-2}$ , explicitly determining the bunch intensity, while in the bottom plot the WP is fixed and the iso-luminosity lines for different scenarios in terms of number of bunches are overlaid.

## PRELIMINARY PERFORMANCE ESTIMATES

Focusing on the third year of Run-III operation when the bunch intensity is foreseen to reach the maximum acceptable value of  $1.8 \times 10^{11} \text{ ppb}$ , preliminary performance estimates along an LHC fill can be seen in Fig. 11. The BCMS beams

provide 2736 collisions in the two high-luminosity experiments, with an initial emittance of  $2.5 \mu\text{m}$ , in the worst case. The transverse emittances during the fill length are evaluated based on the IBS and SR modelling at 7 TeV with the addition of the Run-II observed extra emittance growth of  $0.05 \mu\text{m h}^{-1}$  in the horizontal plane and  $0.10 \mu\text{m h}^{-1}$  in the vertical plane [23]. On the other hand, the bunch length shrinks during the leveling from the initial 1.2 ns to 1.0 ns in 9.4 h and then is kept constant by longitudinally blowing-up the beam. Finally, in order to minimize the triplet irradiation, the crossing angle is adapted while  $\beta^*$  is squeezed down to 0.28 m to provide IP1/5 with constant luminosity of  $2 \times 10^{34} \text{ Hz cm}^{-2}$  (53 events of pileup) for 11.2 h. Assuming a burn-off cross-section of 110 mb to model additional losses and a turnaround time of 4 h, an optimal fill length of 13.8 h results in an integrated luminosity of  $1.31 \text{ fb}^{-1}$  per day.

IBS+SR+Extra Growth of H=0.05  $\mu\text{m/h}$  & V=0.10  $\mu\text{m/h}$ , Leveling at  $2.0 \times 10^{34} \text{ Hz/cm}^2$   
 $N_{1,2} = 1.80 \times 10^{11}$  pbb,  $\phi/2 = 109 \mu\text{rad}$ , nb = 2736,  $\beta_0^* = 1.0$  m,  $\epsilon_{n,Y}^{X,Y} = 2.5 \mu\text{m}$   
 $\sigma_{b,off} = 110$  mb,  $\sigma_{inel} = 81$  mb

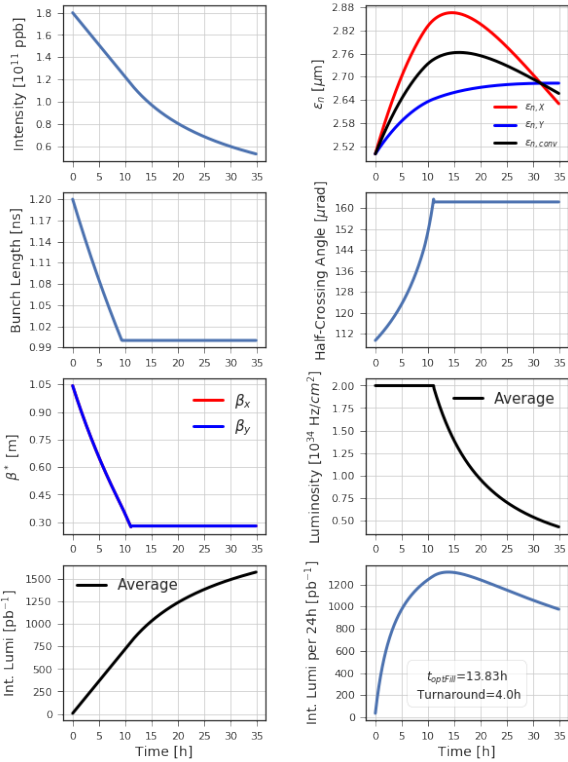


Figure 11: Typical profiles of the evolution of beam and machine parameters during a fill in 2023. The initial conditions of BCMS beams with  $1.8 \times 10^{11}$  pbb bunch intensity,  $2.5 \mu\text{m}$  normalized emittance and 1.2 ns bunch length are applied. The evolution of emittances follow the estimates of IBS and SR with the additional growth, observed during Run-II. The bunch length is leveled when it reaches 1.0 ns.

Leveling for 11 h is novel for the LHC operation and was initially only foreseen for the HL-LHC. To estimate the performance of operating in such a regime, the 2018 run fill

statistics have been used under different scenarios in terms of number of bunches (BCMS or mixed) and initial emittance ( $1.8 \mu\text{m}$  and  $2.5 \mu\text{m}$ ). The estimates, shown in Fig. 12, result in an average integrated performance of  $108 \text{ fb}^{-1}$ , comparing to the  $65 \text{ fb}^{-1}$  of the 2018 run. The values for the average half-crossing angle and  $\beta^*$  at the time of dump are  $122 \mu\text{rad}$  and  $0.55$  m, respectively. The integrated performance is not significantly impacted, within 2 %, between the different scenarios thanks to the leveling.

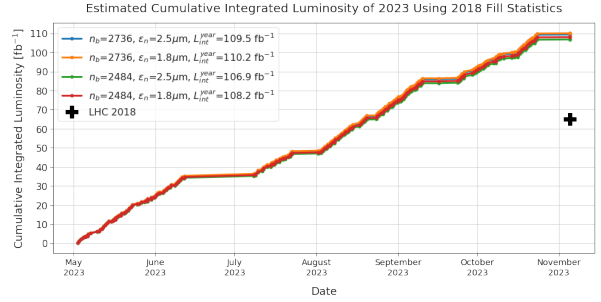


Figure 12: The estimated integrated performance of the 2023 physics production run, using the fill length statistics of 2018. The different scenarios that are considered in terms of initial normalized emittance and number of bunches do not impact significantly the final result, due to the leveling process.

So far the operational scenarios have been focused mainly on the round optics. The flat optics configuration suggested for LHC operation in Run-III [30] has  $\beta_{X^*}^*/\beta_{Y^*}^* = 0.50/0.15$  m. The leveling process is planned to start in round optics mode, squeezing the  $\beta^*$  until the point of 0.50 m, and then while  $\beta_{X^*}^*$  is kept at 0.50 m,  $\beta_{Y^*}^*$  is reduced gradually down to 0.15 m. From the 2018 fill length statistics, only a few fills would reach a  $\beta^*$  that would allow flattening the optics before dump.

In terms of integrated performance, Fig. 13 shows comparative plots of flat optics versus round optics as a function of the leveled luminosity and of the bunch intensity considering the LIU brightness curves. Despite the significantly increased virtual luminosity provided by the flat optics, their integrated performance is limited by the limit on the peak luminosity. At a leveled luminosity of  $2 \times 10^{34} \text{ Hz cm}^{-2}$  the gain in integrated performance with the flat optics is at the level of 1.5 %, arising from the slightly elongated leveling process. Increasing the leveled luminosity, the gain in performance increases almost linearly. In addition, the flat optics can be an appealing option for the first year of Run-III, when the bunch intensity will be relatively low. A gain of integrated performance at the level of  $\approx 7\%$  can be achieved with the flat optics at a bunch intensity of  $1.1 \times 10^{11}$  pbb.

On the other hand, the main benefit of the flat optics comes in the form of lower dose for the inner triplet coils. In Table 1 an assumption is made on the integrated luminosity that can be achieved per year during Run-III and the dose in the limiting magnet coils is estimated for the case of round and flat optics. For the round optics case, with the help of the crossing angle polarity inversion in IP1,  $235 \text{ fb}^{-1}$  can be

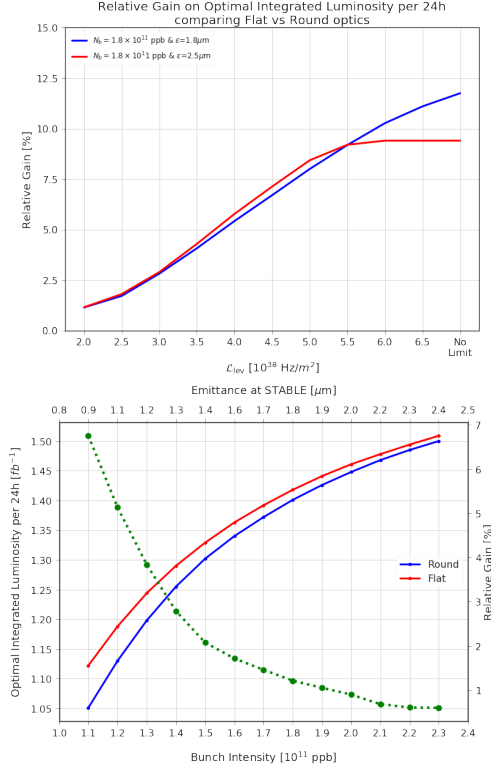


Figure 13: Comparison plots illustrating the potential performance gain of flat optics with respect to round optics as a function of the leveled luminosity (top) and of the bunch intensity (bottom). For the bottom plot a leveled luminosity of  $2 \times 10^{34} \text{ Hz cm}^{-2}$  is considered. In addition, the dotted green curve shows the relative gain in integrated performance between the two optics configurations.

collected before reaching the limit of 30 MGy. Furthermore, adapting the crossing angle within the duration of the fill further reduces the triplet irradiation, allowing for  $15 \text{ fb}^{-1}$  more compared to a situation where the crossing angle would be kept constant to its maximum value of  $162 \mu\text{rad}$ . For flat optics, including a polarity inversion in IP5, a small additional margin is achieved for the IR1 triplets. However, the triplet in IR5 can be preserved in a sizable extend, and therefore used as IR8 spare for the HL-LHC era.

## DESIGNING THE LHC CYCLE

With most of the constraints of the LHC Run-III operation put in place, the campaign of constructing the complete LHC cycle optics has started. To ease the re-commissioning, the round optics are chosen for 2021. Further deliberations on the commissioning of flat optics for 2022/2023 will take place during first YETS of Run-III. The decision will be based on the results of further MD studies, the refined triplet lifetime estimates and performance forecast, as well as the confirmation of the CERN master schedule.

| Run-III prospects                               | LS2 | 2021 | 2022   | 2023   | Total |
|---|-----|------|--------|--------|-------|
| Beam Energy [TeV]                               |     | 7.0  | 7.0    | 7.0    |       |
| $\mathcal{L}_{\text{int}}$ [ $\text{fb}^{-1}$ ] | 190 | 25   | 90     | 120    | 425   |
| ROUND OPTICS                                    |     |      |        |        |       |
| Lumi.averaged half X-angle [ $\mu\text{rad}$ ]  |     | -162 | -148   | +134   |       |
|   |     |      | (-162) | (+162) |       |
| IR1Q2a up [MGy]                                 | 13  | 1.2  | 4.2    | 11.9   | 30    |
|   |     |      |        | (13.4) | (32)  |
| IR1Q2a down [MGy]                               | 11  | 2.8  | 9.5    | 5.6    | 29    |
|   |     |      | (10.0) | (29)   |       |
| IR5Q2b in [MGy]                                 | 11  | 1.9  | 6.2    | 7.5    | 27    |
|   |     |      | (6.8)  | (9.1)  | (29)  |
| FLAT OPTICS                                     |     |      |        |        |       |
| Lumi.averaged half X-angle [ $\mu\text{rad}$ ]  |     | 130  | 130    | 130    |       |
| IR1Q2a up [MGy]                                 | 13  | 1.7  | 6.0    | 8.0    | 29    |
| IR1Q2a down [MGy]                               | 11  | 1.7  | 6.0    | 8.0    | 27    |
| IR5Q2b in [MGy]                                 | 11  | 1.0  | 3.6    | 4.8    | 20    |

Table 1: Forecast of the irradiation dose in the most limiting magnet coils of the IR1/5 triplets for Run-III. The study involves both round and flat optics. In the case of round optics, the adaptive crossing angle scenario is compared to the constant crossing angle one (in parenthesis).

## Optics Constraints & Anti-telescopic Optics

The requirements and the constraints of the different parts of the LHC cycle guide the definition of optics parameters:

- Injection: The optics remains unchanged with respect to 2017/2018 operation;
- Ramp: A change of the beam process is required to allow for a telescopic index in the range of 2-3. Following the LIU intensity ramp-up, a recommissioning of the ramp process is foreseen for the first YETS of Run-III, in order to increase the end of ramp  $\beta^*$ , in a scenario where the beams will be put into collision immediately after the ramp (see below);
- Squeeze: The squeeze beam process will be skipped;
- and replaced by a "Collide and Squeeze" beam process to allow for reducing the  $\beta^*$  in IP1/5 until reaching the maximum luminosity of  $2 \times 10^{34} \text{ Hz cm}^{-2}$ .

During stable beams, IP1/5 will be leveled by simultaneously adapting the crossing angle and the  $\beta^*$  to keep the luminosity constant to  $2 \times 10^{34} \text{ Hz cm}^{-2}$ . The luminosity in the other two experiments will be leveled by offsetting the beams in their respective parallel planes to a target of  $1.3 - 1.4 \times 10^{31} \text{ Hz cm}^{-2}$  and  $2 \times 10^{33} \text{ Hz cm}^{-2}$  for IP2 and IP8, respectively. In addition, the forward physics experiments require the squeeze of  $\beta^*$  in IP1/5 to happen in telescopic mode, since it keeps constant the transfer matrix from the IP to the Roman Pots [31].

The large dynamic range of end-of-ramp  $\beta^*$  and the need of a telescopic index deployed already in the ramp, require



a special optics configuration for the collision process to be matched to ramp and consequently to the injection optics. The range of 1-4 of the telescopic index in terms of optics match-ability, suggests the start of collisions from an anti-telescopic configuration, where the telescopic index ( $r_{ATS}$ ) is inverted to  $1/r_{ATS}$ . This inversion results in an advance of the  $\beta$ -beating wave by one FODO cell, essentially making the strong, in terms of Landau damping efficiency, octupoles of sectors S81/12/45/56 weak and vice versa. This anti-telescopic scheme can therefore define the Combined Ramp and Anti-Telescopic Squeeze (CRATS) scheme, with the collisions starting from an anti-telescope configuration (e.g.  $r_{ATS} = 1/2.5$ ) then, while the  $\beta^*$  is squeezed, cross the  $r_{ATS} = 1$  point at around a  $\beta^*$  of 0.6 m and finally continue the squeeze to 0.28 m in the nominal telescopic configuration. The compatibility of the anti-telescopic optics with the telescopic ones was tested in terms of coherent stability and DA and the results are shown in Fig. 14 and 15, respectively. The stability diagrams are sufficiently large to ensure the stability of all coherent modes, also when considering the detrimental effect of beam-beam interactions with the negative octupole polarity. In addition, the DA results, which include the beam-beam interactions show that anti-telescopic and telescopic optics yield similar results.

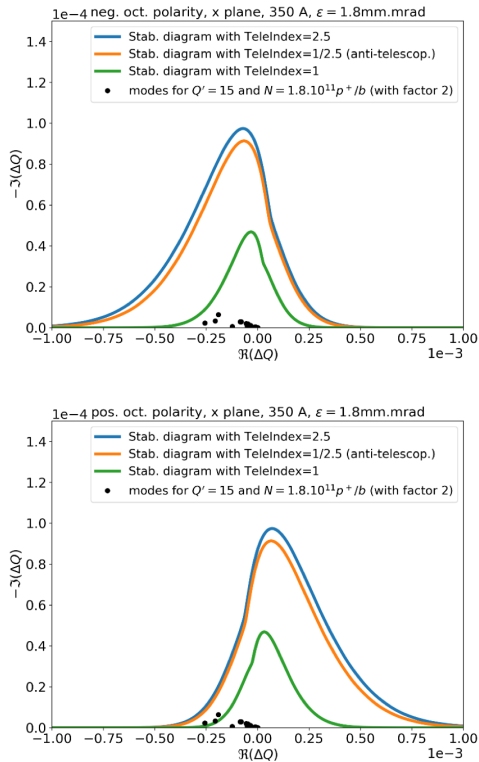


Figure 14: Compatibility tests of the telescopic optics ( $r_{ATS} = 2.5$ ) and the anti-telescopic optics ( $r_{ATS} = 1/2.5$ ) in terms of coherent single-beam stability for both the negative (top) and positive (bottom) octupole polarity. The stability diagrams do not include the beam-beam interactions.

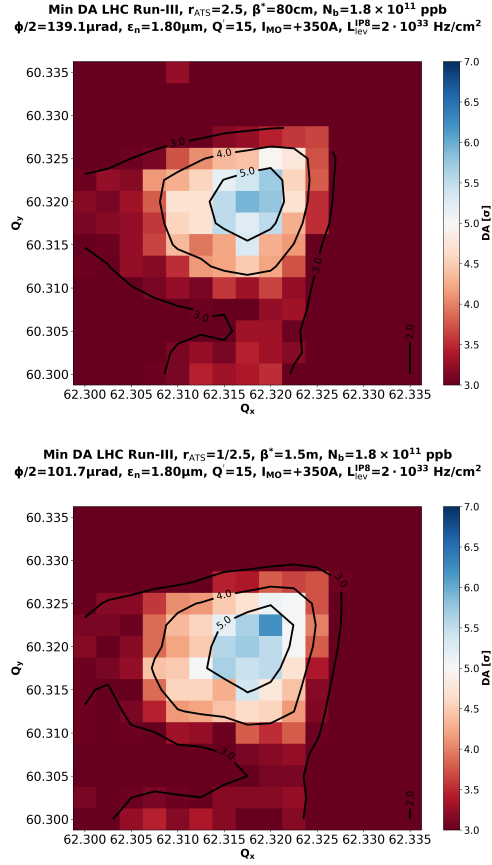


Figure 15: Compatibility tests of the telescopic optics (top) with a telescopic index of  $r_{ATS} = 2.5$  and the anti-telescopic optics (bottom), with index  $r_{ATS} = 1/2.5$ , in terms of dynamic aperture. The simulation includes the effect of the beam-beam interactions. The two optics yield similar results.

## Optics Parameters

With the adoption of the CRATS scheme, the campaign on designing the full LHC optics has already begun and is planned to be finalized by mid-2019. Assuming a re-commissioning of the ramp beam process in the YETS 2021/2022, the beam and optics parameters for the start of collisions (or end of the ramp) for every year of Run-III can be found in Table 2. In addition, the same parameters just before the programmed dump can be found in Table 3 for the round optics and in Table 4 for the flat optics configuration.

## Performance Forecast

Using the optics and beam parameters of Table 2, 3 and 4 and assuming 160 days of physics production with a machine availability of 20% for the first year and 50% for the other two, as well as a turnaround time of 4 h, a performance forecast for every IP and year of Run-III can be estimated. The results, summarized in Table 5, show that 411 (resp. 421)  $\text{fb}^{-1}$  can be collected for IP1/5 using the round (resp. flat) optics. In addition, 216  $\text{pb}^{-1}$  can be collected for IP2. The

|   | 2021                      | 2022                    | 2023                    | Comment  |
|---|---------------------------|-------------------------|-------------------------|--|
| BEAM PARAMETERS @ START OF COLLISIONS                               |                           |                         |                         |  |
| Beam Energy [TeV]   |                           | 7.0                     |                         | To be consolidated   |
| Bunch Charge [ $10^{11}$ ppb]                                       | 0 $\rightarrow$ 1.4       | 1.4 $\rightarrow$ 1.8   | 1.8                     | Following the LIU ramp-up to 2023  |
| Normalized Emittance [ $\mu\text{m}$ ]                              | 2.5                       | 2.5                     | 2.5                     | To allow for extra margin  |
| Bunch Length [ns]   | 1.2                       | 1.2                     | 1.2                     | 1.0 ns at $\approx 10$ h in SB   |
| Collisions in IP1/5 & IP2/8   | 2736 / 2736 & 2250 / 2376 |                         |                         | Assuming BCMS  |
| OPTICS PARAMETERS @ START OF COLLISIONS                             |                           |                         |                         |  |
| $\beta^*$ [m] in IP1/5  | 1.1                       | 1.5                     | 1.5                     | Anti-telescopic optics   |
| $\beta^*$ [m] in IP2/8  | 10/1.5                    | 10/1.5                  | 10/1.5                  | Constant along Run-III   |
| Half X-angle [ $\mu\text{rad}$ ( $\sigma_{\text{beam}}$ )] in IP1/5 | 108 (12.4)                | 102 (13.6)              | 102 (13.6)              | V/H for round, H/V for flat optics   |
| $\mathcal{L}_{\text{peak}}$ in IP1/5 [ $10^{34}$ Hz cm $^{-2}$ ]    | 0 $\rightarrow$ 1.55      | 1.19 $\rightarrow$ 1.98 | 1.19 $\rightarrow$ 1.98 | For best lumi conditions ( $\epsilon_n = 1.8 \mu\text{m}$ )                    |
| Half X-angle [ $\mu\text{rad}$ ] in IP2/8                           | 200/250                   | 200/250                 | 200/250                 | V/H in IP2/8   |
| Half // Separation [ $\sigma_{\text{coll}}$ ] in IP2                | 0 $\rightarrow$ 1.79      | 1.79 $\rightarrow$ 1.89 | 1.89                    | For $1.3 \times 10^{31}$ Hz cm $^{-2}$ and 200-70=130 $\mu\text{rad}$ crossing |
| Half // Separation [ $\sigma_{\text{coll}}$ ] in IP8                | 0 $\rightarrow$ 0.76      | 0.76 $\rightarrow$ 0.97 | 0.97                    | For $2 \times 10^{33}$ Hz cm $^{-2}$ and 250+135=385 $\mu\text{rad}$ crossing  |

Table 2: Beam and optics parameters forecast at the start of collisions (or end of RAMP) for every year of Run-III.

| ROUND OPTICS  | 2021                              | 2022                    | 2023      | Comment  |
|---|-----------------------------------|-------------------------|-----------|--|
| BEAM PARAMETERS @ END OF COLLISIONS                                 |                                   |                         |           |  |
| Bunch Charge [ $10^{11}$ ppb]                                       | 0 $\rightarrow$ 0.89              | 0.89 $\rightarrow$ 0.97 | 0.97      | Following the LIU ramp-up to 2023  |
| Normalized Emittance [ $\mu\text{m}$ ]                              | 2.5                               | 2.5                     | 2.5       | Assuming no emittance evolution  |
| Bunch Length [ns]   | 1.0                               | 1.0                     | 1.0       | 1.0 ns at $\approx 10$ h in SB   |
| Collisions in IP1/5 & IP2/8   | 2736 / 2736 & 2250 / 2376         |                         |           | Assuming BCMS  |
| OPTICS PARAMETERS @ END OF COLLISIONS                               |                                   |                         |           |  |
| $\beta^*$ [m] in IP1/5  | 0.28                              | 0.28                    | 0.28      | Telescopic optics  |
| Half X-angle [ $\mu\text{rad}$ ( $\sigma_{\text{beam}}$ )] in IP1/5 | 162 (9.4)                         | 162 (9.4)               | 162 (9.4) | V/H crossing planes in IP1/5   |
| Leveling time at $2 \times 10^{34}$ Hz cm $^{-2}$ [h]               | 0 $\rightarrow$ 5.0               | 5.0 $\rightarrow$ 11.9  | 11.9      | Burn-off $\sigma_{\text{boff}} = 110$ mb                                       |
| Optimal Fill Length [h]   | 0 $\rightarrow$ 9.8               | 9.8 $\rightarrow$ 14.6  | 14.6      | Assuming 4 h of turnaround   |
| $\beta^*$ [m] in IP2/8  | 10 / 1.5                          | 10 / 1.5                | 10 / 1.5  | Constant along the Run-III   |
| Half X-angle [ $\mu\text{rad}$ ] in IP2/8                           | 200/250                           | 200/250                 | 200/250   | V/H in IP2/8   |
| Half // Separation [ $\sigma_{\text{coll}}$ ] in IP2                | 0 $\rightarrow$ 1.60 <sup>1</sup> | 1.60 $\rightarrow$ 1.64 | 1.64      | For $1.3 \times 10^{31}$ Hz cm $^{-2}$ and 200-70=130 $\mu\text{rad}$ crossing |
| Half // Separation [ $\sigma_{\text{coll}}$ ] in IP8                | 0 $\rightarrow$ 0.13 <sup>2</sup> | 0.13 $\rightarrow$ 0.38 | 0.38      | For $2 \times 10^{33}$ Hz cm $^{-2}$ and 250+135=385 $\mu\text{rad}$ crossing  |

<sup>1</sup> Luminosity leveling at  $1.3 \times 10^{31}$  Hz cm $^{-2}$  in IP2 over the full fill length is granted when the intensity ramp-up reaches  $\approx 2 \times 10^{10}$  ppb with 2250 collisions per turn.

<sup>2</sup> Luminosity leveling at  $2 \times 10^{33}$  Hz cm $^{-2}$  in IP8 over the full fill length will be granted towards the end of 2021 at  $1.4 \times 10^{11}$  ppb for negative IP8 dipole polarity assuming 2376 collisions per turn (and earlier for positive polarity, with 115  $\mu\text{rad}$  internal half-crossing angle, when the intensity ramp-up reaches  $1.15 \times 10^{11}$  ppb).

Table 3: Beam and optics parameters forecast before dump for the round optics scenario, assuming the programmed dump coincides with the optimal fill length for IP1/5.

target of IP8 to collect  $50 \text{ fb}^{-1}$  until LS4 should be exceeded, given the  $31 \text{ fb}^{-1}$  already collected during Run-III.

## CONCLUSIONS

With the completion of the LS2, LHC will restart operation in 2021 for the third run period of physics production. The restart coincides with the completion of the LIU project which offers the opportunity to operate with much brighter beams. After implementing the planned upgrades the LHC will be ready to accept a maximum bunch population of  $1.8 \times 10^{11}$  ppb with an emittance at the start of collisions in the range of 1.8-2.5  $\mu\text{m}$ .

The main guideline for the Run-III operational scenarios is the preservation of the IP1/5 triplet lifetime. This can be achieved by operating close to the beam-beam limit, adapting simultaneously the crossing angle with the tele-

scopic squeeze of the  $\beta^*$  at the two high luminosity experiments during the fill. With this scheme the presently known Squeeze beam process has to be replaced with the Collide and Squeeze one. The other two experiments (IP2/8) are planned to be leveled to their respective luminosity targets using the beam offset leveling.

The large dynamic range of the  $\beta^*$  at the start of collisions and the need to deploy a telescopic index already in the ramp brought forth the idea of anti-telescopic optics. The concept has already been tested in simulations and proved very similar to the telescopic ones in terms of coherent stability and DA. Concerning the optics flavors, round optics is the choice for the year after the restart, while the commissioning of flat optics, which sensibly mitigates the dose deposited in the triplets of IR5, will be decided in the first YETS.

| FLAT OPTICS   | 2021                      | 2022        | 2023       | Comment  |
|---|---------------------------|-------------|------------|--|
| BEAM PARAMETERS @ END OF COLLISIONS                                 |                           |             |            |  |
| Bunch Charge [ $10^{11}$ ppb]                                       | 0 → 0.81                  | 0.81 → 0.87 | 0.87       | Following the LIU ramp-up to 2023  |
| Normalized Emittance [ $\mu\text{m}$ ]                              | 2.5                       | 2.5         | 2.5        | Assuming no emittance evolution  |
| Bunch Length [ns]   | 1.0                       | 1.0         | 1.0        | 1.0 ns at $\approx 10$ h in SB   |
| Collisions in IP1/5 & IP2/8   | 2736 / 2736 & 2250 / 2376 |             |            | Assuming BCMS  |
| OPTICS PARAMETERS @ END OF COLLISIONS                               |                           |             |            |  |
| $\beta^*$ [m] in IP1/5  | 0.50/0.15                 | 0.50/0.15   | 0.50/0.15  | Telescopic optics  |
| Half X-angle [ $\mu\text{rad}$ ( $\sigma_{\text{beam}}$ )] in IP1/5 | 133 (10.3)                | 133 (10.3)  | 133 (10.3) | H/V crossing planes in IP1/5   |
| Leveling time at $2 \times 10^{34}$ Hz $\text{cm}^{-2}$ [h]         | 0.0 → 7.4                 | 7.4 → 14.3  | 14.3       | Burn-off $\sigma_{\text{boff}} = 110$ mb   |
| Optimal Fill Length [h]   | 0 → 10.8                  | 10.8 → 16.4 | 16.4       | Assuming 4 h of turnaround   |
| $\beta^*$ [m] in IP2/8  | 10 / 1.5                  | 10 / 1.5    | 10 / 1.5   | Constant along the Run-III   |
| Half X-angle [ $\mu\text{rad}$ ] in IP2/8                           | 200/250                   | 200/250     | 200/250    | V/H in IP2/8   |
| Half // Separation [ $\sigma_{\text{coll}}$ ] in IP2                | 0 → 1.56 <sup>1</sup>     | 1.56 → 1.59 | 1.59       | For $1.3 \times 10^{31}$ Hz $\text{cm}^{-2}$ and $200 - 70 = 130$ $\mu\text{rad}$ crossing |
| Half // Separation [ $\sigma_{\text{coll}}$ ] in IP8                | 0.0 <sup>2</sup>          | 0.0         | 0.0        | For $2 \times 10^{33}$ Hz $\text{cm}^{-2}$ and $250 + 135 = 385$ $\mu\text{rad}$ crossing  |

<sup>1</sup> Luminosity leveling at  $1.3 \times 10^{31}$  Hz  $\text{cm}^{-2}$  in IP2 over the full fill length is granted when the intensity ramp-up reaches  $\approx 2 \times 10^{10}$  ppb with 2250 collisions per turn.

<sup>2</sup> Luminosity leveling at  $2 \times 10^{33}$  Hz  $\text{cm}^{-2}$  stops at IP8 when the bunch population reaches  $0.88 \times 10^{11}$  ppb with 2376 collisions per turn and negative spectrometer polarity. For positive spectrometer polarity, IP8 levelling conditions are granted down to  $0.71 \times 10^{11}$  ppb, beyond the optimal length for flat optics in 2022/2023.

Table 4: Beam and optics parameters forecast before dump for the flat optics scenario ( $\beta_X^*/\beta_{||}^* = 0.50/0.15$  m), assuming the programmed dump coincides with the optimal fill length for IP1/5.

|  | 2021           | 2022                     | 2023        |
|--|----------------|--------------------------|-------------|
| Bunch Charge [ $10^{11}$ ppb]                            | 0 → 1.4        | 1.4 → 1.8                | 1.8         |
| ROUND (FLAT) OPTICS                                      |                |                          |             |
| Opt. Fill Length [h]                                     | 0 → 9.8 (10.8) | 9.8 (10.8) → 14.6 (16.4) | 14.6 (16.4) |
| $\beta^*$ in IP1/5 [m]                                   |                | 0.28 (0.50/0.15)         |             |
| $\mathcal{L}_{\text{int}}$ in IP1/5 [ $\text{fb}^{-1}$ ] | 18 (19)        | 97 (102)                 | 106 (110)   |
| $\beta^*$ in IP2 [m]                                     |                | 10.0                     |             |
| $\mathcal{L}_{\text{int}}$ in IP1/5 [ $\text{pb}^{-1}$ ] | 36             | 90                       | 90          |
| $\beta^*$ in IP8 [m]                                     |                | 1.5                      |             |
| $\mathcal{L}_{\text{int}}$ in IP1/5 [ $\text{fb}^{-1}$ ] | 3              | 14                       | 14          |

<sup>1</sup> Luminosity leveling at  $1.3 \times 10^{31}$  Hz  $\text{cm}^{-2}$  in IP2 over the full fill length is granted when the intensity ramp-up reaches  $\approx 2 \times 10^{10}$  ppb with 2250 collisions per turn.

<sup>2</sup> Luminosity leveling at  $2 \times 10^{33}$  Hz  $\text{cm}^{-2}$  in IP8 over the full fill length is granted when the intensity ramp-up reaches  $1.4 \times 10^{11}$  ppb (resp.  $1.15 \times 10^{11}$  ppb) with 2376 collisions per turn for negative (resp. positive) IP8 spectrometer polarity. A performance reduction factor of 50 % has been applied accordingly in 2021.

Table 5: Integrated performance forecast for every year of Run-III production period. 160 days of operation are assumed together with a machine availability of 20 % in 2021 (effective over the 160 days) and 50 % for the rest of the run. In terms of turnaround, 4 h are assumed. The intensity ramp-up is assumed to be linear within each individual year.

With all the requirements in place the design of the full LHC cycle optics has already started. Preliminary performance estimates show an integrated luminosity of about  $110 \text{ fb}^{-1}$  for IP1/5 in 2023, when the injected intensity will reach the maximum acceptable target of  $1.8 \times 10^{11}$  ppb.

## ACKNOWLEDGEMENTS

The authors would like to extend their thanks to all colleagues from BE-ABP, BE-RF, BE-OP, EN-SMM, EN-STI, LPC, TE-ABT, TE-CRG, TE-MPE, TE-MSD for their con-

tributions to the discussions that took place within the LHC Run-III Configuration Working Group.

## REFERENCES

- [1] O. Brüning, et al., "LHC Design Report", *CERN Yellow Reports: Monographs*, CERN-2004-003-V1, CERN-2004-003, CERN-2004-003-V-1, 2004.
- [2] H. Damerou, et al., "LHC Injectors Upgrade: Technical Design Report", *CERN Reports*, CERN-ACC-2014-0337, 2014.

- [3] G. Aad, et al., ATLAS Collaboration, "The ATLAS Experiment at the CERN Large Hadron Collider", *JINST*, 3, S08003, 2008.
- [4] S. Chatrchyan, et al., CMS Collaboration "The CMS Experiment at the CERN LHC", *JINST*, 3, S08004, 2008.
- [5] K. Aamodt, et al., ALICE Collaboration, "The LHCb Detector at the LHC", *JINST*, 3, S08002, 2008.
- [6] A. Alves Augusto, et al., LHCb Collaboration, "The LHCb Detector at the LHC", *JINST*, 3, S08005, 2008.
- [7] R. Staszewski et al., AFP Collaboration, "The AFP Project", *Acta Phys. Pol. B* 42, 1615-1624, 2011.
- [8] M. Albrow et al., CMS and TOTEM Collaborations, "CMS-TOTEM Precision Proton Spectrometer", *CERN Reports*, CERN-LHCC-2014-021, TOTEM-TDR-003, CMS-TDR-13, 2014.
- [9] L. Arnaudon et al., "Linac4 Technical Design Report", *CERN Reports*, CERN-AB-2006-084, CARE-Note-2006-022-HIPPI, 2006.
- [10] G. Rumolo et al., "What to expect from the injectors during Run 3", in *Proc. 9th LHC Operations Evian Workshop*, Evian, France, 30-1 January-February 2019.
- [11] G. Apollinari et al., "High-Luminosity Large Hadron Collider (HL-LHC) : Technical Design Report", *CERN Yellow Reports: Monographs*, 4 (2017) 1-516, CERN, CERN-2017-007-M, 2017. ISBN: 9789290834700 (print), 9789290834700 (online).
- [12] R. Steerenberg et al., "Beams from Injectors in 2016, *LHC Performance Workshop*, Chamonix, France, 25-28 January 2016.
- [13] F. M. Velotti et al., "LHC injection system along run II", in *Proc. 9th LHC Operations Evian Workshop*, Evian, France, 30-1 January-February 2019.
- [14] H. Timko et al., "LHC Longitudinal Beam Dynamics in Run-II", in *Proc. 9th LHC Operations Evian Workshop*, Evian, France, 30-1 January-February 2019.
- [15] H. Timko et al., "Estimated LHC RF system performance reach at injection during Run-III and beyond", *CERN Accelerator Notes*, CERN-ACC-NOTE-2019-0005, 2019.
- [16] G. Ferlin et al., "Cryogenics experience during Run2 and impact of LS2 on next run", in *Proc. 9th LHC Operations Evian Workshop*, Evian, France, 30-1 January-February 2019.
- [17] C. Bracco et al., "LBDS Performance in Run II", in *Proc. 9th LHC Operations Evian Workshop*, Evian, France, 30-1 January-February 2019.
- [18] A. Perillo-Marcone et al., "LHC Dump Assembly – Operational Feedback and Future Prospective", in *Proc. 9th LHC Operations Evian Workshop*, Evian, France, 30-1 January-February 2019.
- [19] J. Maestre Heredia, et al., "TCDQ thermo-mechanical analysis for the HL-LHC", in *7th LHC Run-III Configuration Working Group Meeting*, CERN, Geneva, Switzerland, 9 November 2018.
- [20] D. Missiaen, "Realignment around CMS", *363rd LHC Machine Committee*, CERN, Geneva, Switzerland 3 October 2018.
- [21] N. Fuster-Martinez et al., "Collimation", in *Proc. 9th LHC Operations Evian Workshop*, Evian, France, 30-1 January-February 2019.
- [22] F. Antoniou et al., "Building a luminosity model for the LHC and HL-LHC", in *Proc. 6th International Particle Accelerator Conference (IPAC 2015)*, Richmond, Virginia, 3-8 May 2015.
- [23] N. Karastathis et al., "Monitoring and Modeling of the LHC Luminosity Evolution in 2017", *J.Phys.Conf.Ser.*, 1067 no.2, 022006, 2018.
- [24] G. Iadarola et al., "Electron cloud and heat loads", in *Proc. 9th LHC Operations Evian Workshop*, Evian, France, 30-1 January-February 2019.
- [25] D. Boussard et al., "The LHC Transverse Damper (ADT) Performance Specification", *CERN Reports*, CERN, SL-Note-99-055-HRF, 2000.
- [26] S. Fartoukh, "Achromatic telescopic squeezing scheme and application to the LHC and its luminosity upgrade", *Phys. Rev. ST Accel. Beams*, 16, 111002, 2013.
- [27] F. Cerutti et al., "LHC triplet lifetime versus operational scenario in ATLAS and CMS", in *225th LHC Machine Committee*, CERN, Geneva, Switzerland, 8 July 2015.
- [28] S. Fartoukh, "Flat beam Optics", in *19th LHC Machine Advisory Committee*, CERN, Geneva, Switzerland, 15-17 June 2006. <http://mgt-lhc-machine-advisory-committee.web.cern.ch/mgt-lhc-machine-advisory-committee/lhcmac19/Agenda.htm>
- [29] N. Karastathis et al., "Crossing Angle Anti-Leveling at the LHC in 2017", *J. Phys. Conf. Ser.*, 1067, no.2, 022004, 2018.
- [30] S. Fartoukh et al., "About at telescopic optics for the future operation of the LHC", *CERN Reports*, CERN-ACC-2018-0018, 2018.
- [31] C. Royon et al., "The AFP and PPS projects", *Int. J. Mod. Phys.*, A29, no.28, 1446017, 2014.